Załącznik 2

High Level Trigger of the ATLAS experiment at the LHC

dr inż. Tomasz Bołd

Department of Physics and Applied Computer Science
AGH UST Kraków
Al. Mickiewicza 30
30-059 Kraków

Kraków, April 4, 2017

Contents

1 Main research achievement

Research achievement mentioned is development of ATLAS High Level Trigger described in a monograph "High Level Trigger role in extending physics reach of the ATLAS experiment at the LHC - system design and performance" [1]. It was published in the form of a book by the Expol Publishing house with the ISBN 978-83-65256-07-2.

1.1 Introduction

Modern experiments with hadron colliders are constructed to look for very rare processes in the high background environment. For example, the measured, inclusive cross-section for Higgs boson production equals to $33.0 \pm 5.3(stat) \pm 1.6(sys)pb$ [2]. Taking into account experimental convenience of decay channels, the observed frequency is additionally reduced by the branching ratio and detector acceptance. In consequence, in order to perform statistically relevant observation, it is required that the collisions are performed at high energy and with a high luminosity. This, in turn, due to the 9 orders of magnitude higher background cross-section ($\sigma_{pp}^{\text{tot}} = 98.3 \pm 0.2(stat) + 2.8(sys)mb$ [3]), requires application of sophisticated events filters during data taking, called trigger systems. Their purpose is to retain events with rare but interesting signatures with a high efficiency and nearly completely remove the unwanted background events.

1.2 The LHC accelerator and ATLAS experiment

The Large Hadron Collider (LHC) is located in the European Centre for Nuclear Research, CERN, near Geneva. The LHC collides head to head protons with nominal centre of mass energy 14 TeV and luminosity $10^{34}cm^{-2}s^{-1}$. Protons are grouped in 3564 bunches and led to a collision every 25 ns. With the nominal luminosity, in every bunch crossing, about 50 elementary collisions take place (this effect is called pile-up). At lower luminosities lead ions or lead ions with protons are collided a the LHC. In four points of beam interactions four main experiments are located. The LHCb [4] devoted to the CP symmetry breaking measurements, the ALICE [5] designed to suit best heavy ion program and two bigger, general purpose detectors, CMS [6] and ATLAS [7].

An innermost part of the ATLAS detector is built from silicon pixel detector (PIXEL), silicon strips (SCT) and transition radiation detector (TRT). These three parts, collectively called Inner Detector (ID), are immersed in 2

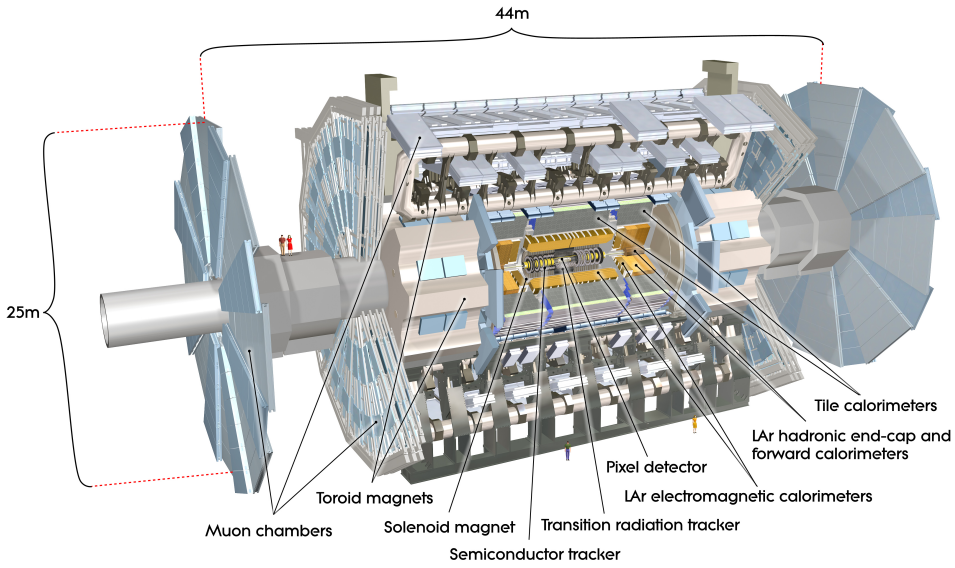

Figure 1: A cross-section view of the ATLAS detector [7].

Tesla magnetic field generated by the superconducting solenoid. The main purpose of the ID is to measure trajectories of the charged particles and indirectly positions of the interaction vertices. The energy of the EM particles is measured in the sampling, lead-liquid-argon (LAr) electromagnetic calorimeter. Energy of hadrons is measured in the steal-plastic sampling, tile calorimeter (Tile) located further away from the interaction point. Trajectories of muons, passing through the layers of calorimeters are detected in the muon spectrometer (MS) in a field of an air core, superconducting, toroidal magnet. A sketch of the detector is shown in Figure 1.

1.3 The role of the online filter system in the ATLAS experiment

The electronically read ATLAS detector channels in nominal conditions generate a stream of data of order of PetaBytes/s. Contemporary data handling technologies disallow recording and then analysis of such data volumes. However, due to the fact that the interesting processes are characterised by a very small cross section rejection of most of the collisions event does not influence experimental reach if only the background is rejected. During filtering per-

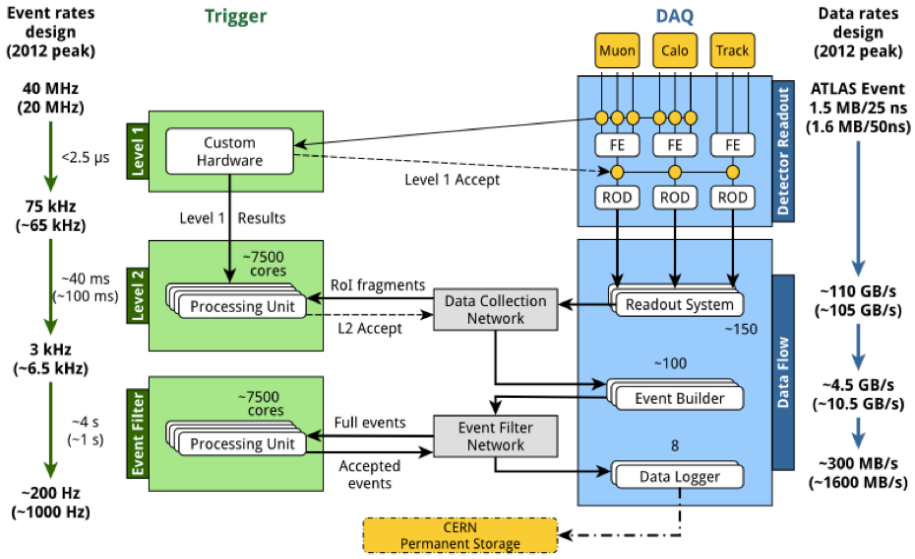

Figure 2: A diagram of the ATLAS Trigger and Data Acquisition System used during data taking in 2010-2013 (so called LHC Run 1) [8].

formed on-line (synchronously with the data taking) a number of events is reduced from 40 MHz down to hundreds of Hz (e.g. 200 Hz in 2011 and 1 kHz in 2016). A schematic diagram of the ATLAS Trigger and Data Acquisition system is shown in Figure 2. The trigger part (left) consists of the hardware low-level system (L1) and precise, software High Level Trigger (HLT).

The L1 filter consists of two subsystems dedicated to finding signals in calorimeters (L1Calo) and muon spectrometer (L1Muon). Time to take the decision by the L1 is determined by the depth of the derandomizing buffers in the detector front-end electronics and is as small as 2.5 μs. Due to that the L1 performs only a very coarse selection.

In the L1Calo signals from the calorimeter cells are aggregated into so-called trigger towers of a dimension $\eta \times \phi = 0.1 \times 0.1$ and a local maximum is searched in groups of 2×2 towers for electromagnetic objects or bigger for hadronic jets, collimated sprays of hadrons. For the maxima, the transverse energy is estimated from the towers as well as the deposition in the proximity used to estimate the isolation level.

Muons are found by looking for signals from detector chambers wired so that a particle emitted from an interaction region results in a coincidence of

the signals. By controlling the wiring and a number of signals required in the coincidence, the L1Muons provide, an estimate of the muon momentum.

A Central Trigger Processor (CTP) of the L1 system receives the information about objects multiplicity and thresholds from L1Calo and L1Muon and combines them into logical expressions (256 in 2010-2015 and 512 now). A logical sum of this expressions defines the fate of the event. This is, any expression yielding a positive results makes an event considered for further selection. The results of CTP decisions and positions of objects identified by L1Muons and L1Calo, the Regions of Interest (RoIs) are passed to HLT. For events accepted by the L1, up to 100 kHz, an information from on-detector frontend electronics is moved to the Readout System (RoS) characterised by deeper memory buffers from where the event data is provided to the HLT for further analysis.

The HLT is a farm of about 40000 CPU cores (in 2015-2016) which is responsible for precise filtering of collision events and rate reduction. In years 2005-2010 I was major contributor to the design, implementation and deployment of the HLT software.

1.4 The ATLAS HLT system

1.4.1 Main design goals

The role of the HLT is to select 1% of events accepted by the L1 which are recorded for further offline analysis. Every event is tested for many (currently about 2000) various signal hypothesis. Nonetheless the filtering process has to be efficient to avoid the RoS system overflowing causing data losses.

For this reasons, two basic concepts are built in the system at the design stage. Signal hypothesis testing is divided into small steps consisting of reconstruction and hypothesis verification algorithms. They are ordered from computationally simple to more advanced. At each step the partial hypothesis is verified and if it fails further processing is abandoned. This way computational cost is reduced for all rejected events and since these are 99% of all processed events, a significant optimisation is achieved. This approach is called the early rejection.

The ATLAS TDAQ architecture assumes 100 kHz of L1 acceptance rate while at the same time due to the technological and economical limitations, the RoS system allows for readout of the data with about 30 kHz [1]. Therefore, the filtering process at the HLT has to happen with the use of a fraction

[1] The RoS system is gradually upgraded and at the moment some parts of it support event data readout at the full L1 frequency.

of the detector data only. To realise this in practice for most of the signatures the reconstruction process is performed only in RoIs identified by the L1. Typically about 2-5% of detector data is needed at HLT to reject the event. Reconstruction in RoIs is another pillar of the HLT design.

1.4.2 HLT architecture

In years 2010-2013 the HLT system was composed of two parts, the second level filter (L2) where the reconstruction was solely performed in RoIs and so-called event filter (EF) where, on fully built events, the global signatures were tested. Longer time allotted at the EF allowed for the use of a more precise reconstruction borrowed from the offline. In the LHC technical break in 2013-2105 the architecture of the HLT, shown in Figure 2, was simplified by merging the L2 and EF into a uniform HLT system. Functionally, however, the HLT remained the same. In first steps, fast, trigger specific algorithms are executed, followed by event building and precise algorithms execution.

The HLT process consists of the steering algorithm controlling thousands of algorithms specific for each signature. Aforementioned design principles, such as the early rejection and RoIs based reconstruction are implemented by the steering. Thanks to that, the specific algorithms are insulated from the complexity of the reconstruction process. For the flexibility of constructing complex signatures an efficient, graph-based, data exchange system was built in. In addition, it allows for recording of every partial decision taken during the selection and thus facilitating data analysis. Concentrating an extensive functionality in the steering algorithm allows for many optimisations. Among them is the avoidance of repeated reconstruction of RoI required by many hypotheses verified for an event (caching). An influence of such optimisations, not the most critical, though, is shown in Figure 3. This particular optimisation resulted in the reduction of the average execution time by about 30% and therefore allows for application of more time demanding algorithms improving the physics output out of the HLT.

An important aspect of the online filtering is the reliability. In contrary to the offline reconstruction process the filtering process can not be repeated on events which have been rejected. For this reasons the HLT system was equipped with an infrastructure for error detection. In cases of erroneous behaviour the filtering proces is stopped and the event directed to a separate output stream for detailed investigations. Since the most frequent reason for misbehaviour online is an excessive execution time, repetition of the selection process offline with an unlimited time allows for recovering of the HLT decision. Recovered events are integrated with the remaining events

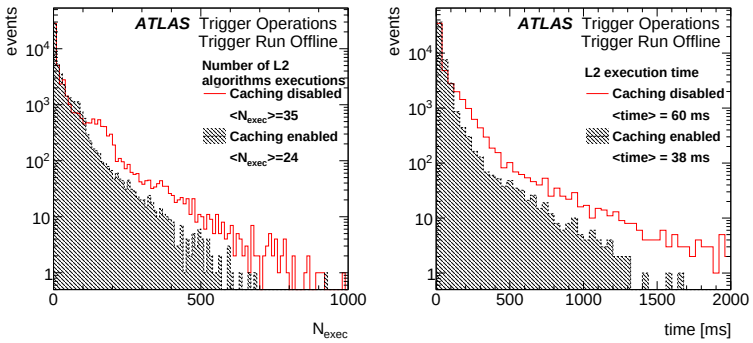

Figure 3: (left) Number of HLT algorithms executions per event with and without the caching optimisation. (right) Total HLT execution time per event with and without the caching optimisation [1].

for analysis which makes the HLT system lossless.

The HLT allows also for an extensive monitoring in real time during the selection. In addition to the operational parameters like rates of each signature, execution times, also all physical parameters available during the reconstruction and hypothesis validation like RoI positions, particles momenta etc. are exposed in a form of the histograms during the data taking. These histograms are then monitored by automated data quality systems and data tacking crew [1] (in chapter 4).

Components of described system were created in 2006-2010 with my significant contribution or under my supervision.

1.4.3 HLT deployment and evolution

The data taking at the LHC started in 2010 at the 7 TeV centre-of-mass energy per proton pair. The ATLAS trigger system was deployed in several steps. Initially, it was operated in a mode when all collisions were recorded. For that reason, the first subsystem which was commissioned for the operation was the L1. At this stage, the HLT was only responsible for splitting the data stream into events originated from calorimeter and muon L1 triggers. The first HLT filter which was enabled online was used to select inelastic collisions. For that, tracking reconstruction algorithms were used and the selection required at least one track found to record the event. The moment when this HLT filter was enabled is shown in Figure 4. The acceptance of the L1 seed was raised and at the same time the HLT enabled filtering accepting $\sim 1‰$ of the input rate.

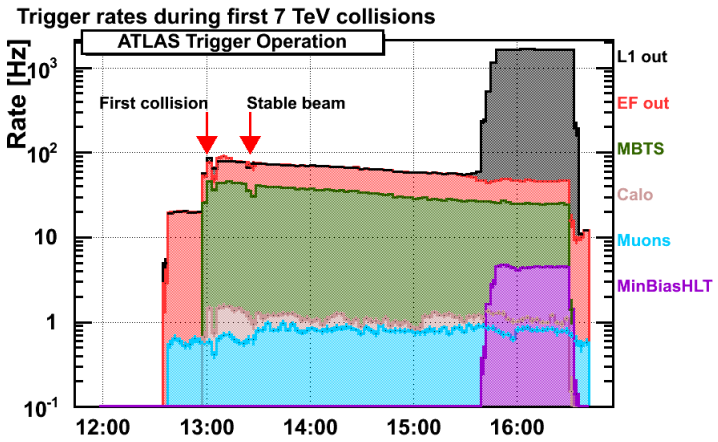

Figure 4: Selected recording rates as a function of time during the first run in which the HLT was enabled in 2010 (change of the rate ∼15:30) [1](chapter 5).

Subsequently, the HLT filtering was deployed in a three-staged procedure. Firstly, the HLT algorithms were executed on recorded earlier data and certified to process the event data without failures. In the next stage, they were run online but with hypothesis algorithms enforced to always accept the events and finally the rejection was enabled. In the middle of 2010 at the luminosity of $\mathcal{L} \simeq 1 \cdot 10^{30} cm^{-2}\mathrm{s}^{-1}$ the initial configuration was replaced by the first physics menu. The menu contained triggers filtering muons, electrons, photons, taus, jets and missing transverse energy as well as special filters for low mass dilepton resonances. With increasing luminosity, the thresholds for inclusive triggers were raised as well as the selection criteria were made stricter. This process is illustrated for example signatures in Table 1.

During these initial years of trigger operation, I was based at CERN and participating in the deployment as a responsible for its correct functioning and initial evolution. In particular, I developed the first version of the system allowing to construct large trigger configurations, so-called trigger menus.

Further evolution of the HLT was determined by growing luminosity which was gradually raised to $\mathcal{L} \sim 8 \cdot 10^{33} cm^{-2}\mathrm{s}^{-1}$ at the end of 2012 (to be compared with design $\mathcal{L} = 10^{34} cm^{-2}\mathrm{s}^{-1}$) and a slight increase of the energy of protons from 7 to 8 TeV greatly increasing pile-up effects. Negative influence harsher conditions on the HLT were mostly concentrated on signatures where the summation of deposits from larger volumes of the calorimeter are

Luminosity [$cm^{-2}s^{-1}$]	$3 \cdot 10^{30}$	$2 \cdot 10^{31}$	$2 \cdot 10^{32}$
Signature	threshold [GeV],selection		
Inclusive			
muon	4	10	13,tight
electron	10,medium	15, medium	15, medium
photon	15,loose	30,loose	40,loose
tau	20,loose	50,loose	84,loose
jet	30	75,loose	95,loose
Inne			
di-muon	4	6	6,loose
di-electron	3,loose	5,medium	10,loose
di-photon	5,loose	15,loose	15,loose

Table 1: Main filters used in 2010. In the table only the lowest thresholds are shown for which all events were recorded at a given luminosity. The selection specified denotes background rejection strength of the filter. For instance "tight" denotes very little background in the selected events while "loose" is allowing for more background events [1] (chapter 5).

required like QCD and tau jets or missing transverse energy. To a lesser extend the signatures with the charged particle tracks were affected. However, the track reconstruction became more difficult due to the higher number of combinations in the initial stage of track seeding which in turn resulted in a slightly reduced efficiency with increased execution time. The example of the influence of the pile-up effect on electron and missing transverse energy triggers is illustrate in Figure 5.

Meanwhile, in 2010 the heavy-ion program was started at the LHC. Initially at the centre-of-mass energy 2.76 TeV per nucleon pair and very low luminosity of $\mathcal{L} \simeq 3 \cdot 10^{25} cm^{-2}s^{-1}$. Therefore in the first heavy-ion run it was sufficient to use the L1 system solely to record all the data. However, already in 2011 and during the following ion runs filtering at the HLT was necessary due to the luminosity increase to $\mathcal{L} \simeq 5 \cdot 10^{26} cm^{-2}s^{-1}$ which made the recording of all collisions impossible. Also, during the proton-lead runs at the end of 2012, the HLT was actively used to select events.

During the heavy-ion data taking, even at small luminosity, in events when the collision happens with a small impact parameter (central collisions) multiplicity of produced particles reaches values higher than during high luminosity proton-proton collisions. In contrary to the pile-up, an average correction of the signals in the detectors can not be used. Instead, the

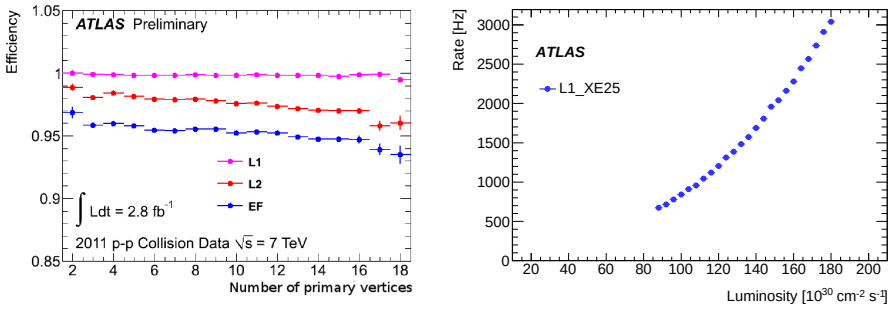

Figure 5: (left) Influence of the pile-up estimated by a number of reconstructed vertices on the electron trigger efficiency. (right) Luminosity dependence of the L1 missing transverse energy trigger rate. A linear dependence is expected for a stable trigger.

corrections have to be established for a particular event. Already in 2011 the hadronic jets reconstruction at the HLT contained a step correcting to an average deposit of low momenta particles. Neglecting of this corrections would have resulted in a bias in the application of a threshold and thus in the recording of events biased towards more central ones. During the heavy-ion run in 2015 ($\mathcal{L} \simeq 1.5 \cdot 10^{27} cm^{-2} s^{-1}$) and energy $\sqrt{s_{NN}} = 5.02$ TeV the aforementioned effects influenced not only jets but all calorimeter based HLT signatures. Since HLT filtering of electromagnetic signatures was required the corrections for an "underlying event" had to be also applied to them. The correction allowed to recover discriminating power of shower shape variables and allowed to construct highly efficient filters as shown in Figure 6.

From the first run in 2010 of the data taking, I was coordinating preparation and operation of the trigger system for heavy-ion runs.

1.4.4 Overview of the trigger strategies implemented in HLT

From the point of the type of reconstruction the HLT filters can be divided into RoIs based, sub-detector based or hybrid ones.

Important for the ATLAS experiment physics program are lepton filters: electrons, muons and taus. Consequently, most of the bandwidth is allocated to them and they consume most of the HLT resources. Their goal is to deliver a sample of events rich in electroweak mediating bosons $W^{\pm}$ and Z^0 of key importance in Standard Model measurements, including the Higgs boson discovery. Algorithms in these filters perform a multistage reconstruction in RoIs defined by the L1 system. In the case of electrons in the earliest

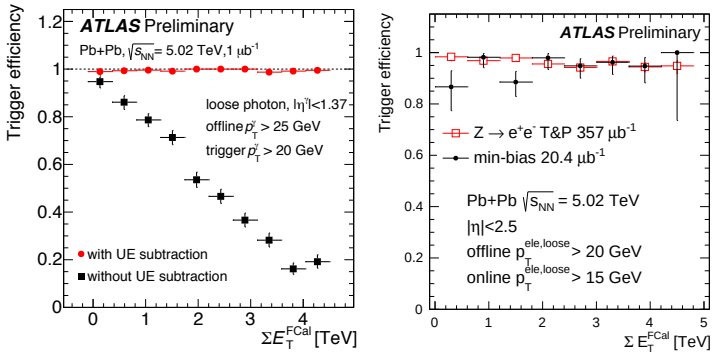

Figure 6: (left) Efficiency of the photon trigger during Pb-Pb run in 2015 as a function of collision centrality proxied by the transverse energy deposit in the forward calorimeter. Two triggers are compared, the one containing correction for the underlying event (red points) and the p-p one (black points). (right) Efficiency for the electron trigger in the same data taking period measured with two methods [1](chapter 5).

stage, the electromagnetic cluster is reconstructed. In addition to the total transverse energy of the cluster, shower shape variables used in background rejection are extracted. A similar procedure is applied to the candidate RoIs with the tau leptons. For muons in the first stage the reconstruction of the tracks in the MS and an extrapolation back to the interaction region is performed. In the next stage, a fast tracking is performed in order to construct a more robust discrimination from the background. Such an order of the reconstruction allows for the application of the partial hypotheses solely on the cluster quantities or standalone MS track and rejection of some RoIs before the CPU expensive ID tracking is performed. This is an example of the early rejection principle application. Upon confirmation of the hypotheses the same steps are repeated with more precise offline-like algorithms. Figure 7 shows efficiencies of example muon and electron triggers.

The evolution of lepton trigger was driven by the need to maintain high efficiency for electroweak bosons. Initially, with raising luminosity the momentum threshold was raised to about 25 GeV. At yet higher luminosities the threshold remained in the region allowing high acceptance but in order to keep rates under control, the selection criteria was tightened. This strategy is not implemented for inclusive tau triggers as the differentiation from the significantly more abundant background hadronic jets is not sufficient to reduce the rate sufficiently. An important group of leptonic triggers are com-

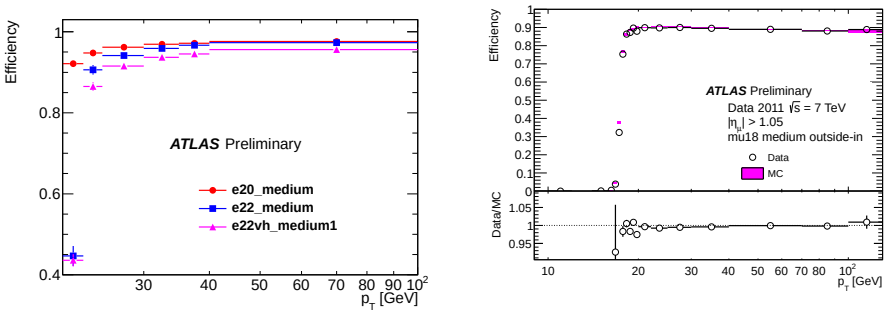

Figure 7: (left) Efficiency of the selected electron HLT filters used in 2011 as measured in data. (right) Comparison of data and MC estimates of the muon filters efficiency in 2011. The cumulative efficiency of L1 and HLT is shown for the endcap muon chambers. In the barrel, he L1 efficiency is smaller by about 15% due to the effect of geometric acceptance of the trigger chambers [1](chapter 5).

binations of two objects. They allow reduction of the momentum thresholds or loosening the selection and thus offer higher signal efficiency.

A photon trigger, also RoIs based, provides a sample of events used for new physics searches as well as precise QCD tests and calibration of hadronic jets reconstruction. A di-photon trigger is used to collect precious events with the direct Higgs boson decay $h \to \gamma\gamma$, which was of a key importance in the discovery. During photons reconstruction the same calorimetric algorithms are used as in case of electrons however the hypothesis algorithms have adjusted criteria for photon initiated electromagnetic cascades [1](chapter 5).

A second important group of filters is based on the information from entire subdetectors of ATLAS. The neutrino (or other weakly interacting particles) triggers use missing transverse energy proxying the missing transverse momentum. The missing transverse energy in the trigger was initially calculated as a vector sum of transverse energies from all calorimeter cells, however, this method, as mentioned earlier, was found to be susceptible to the pile-up effects already at the luminosities of $\mathcal{L} \simeq 1 \cdot 10^{32} \mathrm{c}m^{-2}\mathrm{s}^{-1}$ and more robust techniques were derived. Besides the inclusive missing transverse energy trigger the menu contains many combinations with additional signatures, like a presence of the lepton. An example efficiency of the missing transverse energy trigger is shown in Figure 8.

An important trigger during the early data taking was so-called minimum-bias trigger aiming at efficient recording every inelastic p-p col-

lision. These filters are important in all inclusive measurements however they are of special importance in the heavy-ion program where near 100% efficiency of the entire centrality spectrum allows, above all, for precise centrality calibration. Interaction triggers are based on the signals from the Minimum Bias Trigger Scintillators (hodoscopes located in the forward directions). The efficiency of these triggers is verified by measuring the coincidence rate with the tracks reconstructed in the ID on randomly selected collision bunch crossings. In runs with a small luminosity, such a sample is achieved by applying an additional HLT filtering in which the tracks are searched in the entire ID.

In HLT it is also possible to perform a hybrid reconstruction where both of above-mentioned approaches are interleaved. The main trigger of this kind is used to select events with hadronic jets. The purpose of these triggers is to select events with QCD jets, mostly of a very high momentum or high multiplicity. Specialised inclusive jet samples are recorded for background studies for all calorimetric signatures. The reconstruction in HLT may be performed in several variants. Initially, it was performed in RoIs then the EF reconstruction switched to use entire calorimeter information. Currently, the full calorimeter scan for jets is performed at HLT in the earliest stage already. Both approaches give very similar results for inclusive jets however, differ in multi-jet signatures, the full scan provides a better efficiency even if coarse granularity calorimeter information is used as shown in Figure 8.

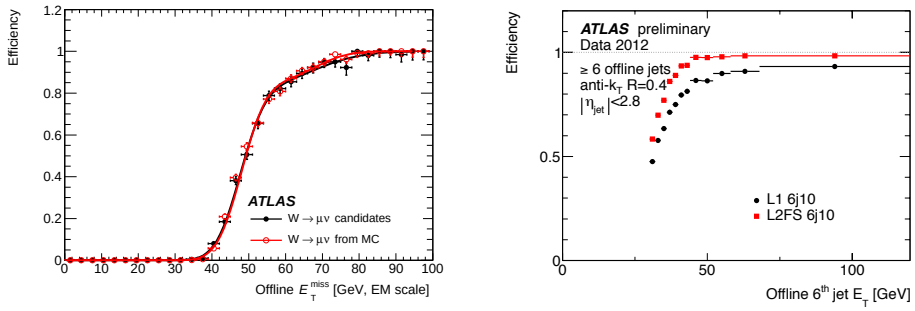

Figure 8: (left) Efficiency of the missing transverse energy filter in 2011 measured in data and MC. (right) Comparison of the multi-jet trigger efficiencies with the reconstruction based on a sliding window algorithm (hardware reconstruction at the L1) (black points) and an application of the anti-k_T algorithm to the same calorimeter information at HLT (red points) [1](chapter 5).

An inverted approach is used in the b-jet triggers. A major challenge, in this case, is a precise secondary vertex reconstruction, where b-hadrons decay initiating hadronic cascade evolution. In contrary to the offline where the complete ID tracking is performed prior to the b-jet identification in online conditions the primary vertex information is not available. In currently operating b-jet triggers in the first reconstruction stage all jets are reconstructed. Within each jet cone tracking with a high transverse momentum track threshold is performed in order to provide tracks for the primary vertex finding. Once the primary vertex is found, for each b-jet candidate a more precise tracking is executed to find the secondary vertex which is an input to the b-jet tagging routines.

Several filtering strategies are presented in order to illustrate the functionality of the HLT system. A more complete description can be found in the monograph "High Level Trigger role in extending physics reach of the ATLAS experiment at the LHC".

It should be made clear that design, implementation, deployment and in particular, the maintenance of the HLT is possible thanks to an effort of a numerous ATLAS collaboration members, especially in the area of optimisations of particular signatures. Nonetheless, me and my two closest collaborators in HLT were awarded of the "ATLAS Outstanding Achievement Award" *"For exceptional work as the chief architects responsible for the design, implementation, commissioning and tireless support of the ATLAS Trigger Core Software."*

1.4.5 HLT Trigger upgrade

In order to maintain high triggering efficiency and selectivity at the High Luminosity LHC (HL-LHC) with $\mathcal{L} \simeq 5 \cdot 10^{34} cm^{-2} s^{-1}$ after the upgrade planned to finish in 2026 some of the ATLAS detectors will be replaces. Also, the Trigger and DAQ systems have to be modernised. First of all the hardware part of the trigger will be upgraded to maintain selectivity in the high pile-up conditions (about 200 interaction per bunch crossing). Also, the HLT will be modernised. A main motivation of the upgrade is to maintain high signal acceptance for inclusive lepton triggers with thresholds suitable for selection of electroweak bosons, this is ∼25 GeV for electrons and muons and ∼30-40 GeV for di-tau triggers. Similarly for photons, multi-jets or b-jets high luminosity with fixed output rates would necessitate an increase of thresholds and thus reduction of signal acceptance.

A few variants of the TDAQ architectures are considered at the moment in which rate of the hardware level is as high as 400 kHz or even 1 MHz from

which the HLT selects events at the rate of up to 10 kHz [9].

An efficient filtering in the conditions of high pile-up and rates and the limited size of the HLT farm is a computational challenge. Achieving high purity of recorded data is only possible after use of highly specialised offline algorithms which need to be integrated into HLT. An increase of the throughput at the HLT goes in concert with a similar effort for the offline reconstruction. Profiting from that an upgraded HLT software will adhere closer to the offline model. As a result deployment in HLT of highly sophisticated offline algorithms which deliver necessary rejection will be streamlined.

The timescale of the HLT upgrade has to adhere to the LHC and ATLAS shutdowns. Therefore in the first step, the modernisation of the HLT framework is planned in two steps. Firstly the framework will be replaced by one common for offline reconstruction and HLT and secondly the major rework of algorithmic code will take place [10]. Completion of the first stage is planned for the year 2020 while till 2026 the improvements in the algorithmic code is expected so that the HLT system is capable of high-efficiency filtering when HL-LHC becomes operational. One of considered options to increase HLT farm computational power is to use external co-processors (GPUs) in some compute dominated algorithms like tracks reconstruction.

I am co-responsible for coordinating the HLT software upgrade effort.

References

[1] T. Bold. *High Level Trigger role in extending physics reach of the ATLAS experiment at the LHC*. Number 978-83-65256-07-2. EXPOL, 2016.

[2] ATLAS Collaboration. Measurements of the Total and Differential Higgs Boson Production Cross Sections Combining the $H \to \gamma\gamma$ and $H \to ZZ* \to 4l$ Decay Channels at $\sqrt{s}$=8 TeV with the ATLAS Detector. *Phys. Rev. Lett.*, 115(9):091801, 2015.

[3] G. Antchev, P. Aspell, I. Atanassov, V. Avati, J. Baechler, et al. First measurement of the total proton-proton cross section at the LHC energy of $\sqrt{}$ s =7 TeV. *Europhys. Lett.*, 96:21002, 2011.

[4] Jr. Alves, A. Augusto et al. The LHCb Detector at the LHC. *JINST*, 3:S08005, 2008.

[5] ALICE Collaboration. Performance of the ALICE Experiment at the CERN LHC. *Int.J.Mod.Phys.*, A29:1430044, 2014.

[6] CMS Collaboration. The CMS Experiment at the CERN LHC. *JINST*, 3:S08004, 2008.

[7] ATLAS Collaboration. The ATLAS Experiment at the CERN Large Hadron Collider. *JINST*, 3:S08003, 2008.

[8] R. Bartoldus et al. Technical Design Report for the Phase-I Upgrade of the ATLAS TDAQ System. Technical Report CERN-LHCC-2013-018. ATLAS-TDR-023, CERN, 2013.

[9] S. George, B. Petersen, E. Lipeles, M. Ishino, N. Konstantinidis, J. Adelman, D. Sankey, T. Pauly, J. Zhang, J. Baines, T. Bold, G. Lehmann Miotto, N. Gee, C. Bee, D. Francis, and D. Strom. Initial Design Review for the Phase-II Upgrade of the ATLAS TDAQ System. Technical Report ATL-COM-DAQ-2016-028, CERN, 2016. (ATLAS internal documentation).

[10] J. Baines, T. Bold, P. Calafiura, S. Kama, C. Leggett, D. Malon, G. A. Stewart, and Wynne B. M. ATLAS Future Framework Requirements Group Report. Technical Report ATL-SOFT-PUB-2016-001, CERN, 2016.

2 Other research

In the hypothesis formulated by J.D. Bjorken in 1980's at sufficiently high temperature ($\sim 10^{12}K$) occurring in relativistic heavy ion collisions can produce so called Quark Gluon Plasma (QGP).

Research on this new state of matter is of interest for several reasons. One of them is a confirmation of the asymptotic freedom in strong interactions which in turn is a contribution to understanding of QCD or even string theories [1]. Conditions created in the laboratory during the these collisions reproduce conditions in the Universe a few microseconds after the Big Bang.

Initially the QGP was assumed to resemble the ideal gass of hadrons. However, results of experiments at performed at Relativistic Heavy Ion Collider indicated that the QGP is more similar to an ideal liquid [2]. Existence of long-range correlations, observed in the final states, is one of the striking signatures of QGP. These correlations are correctly described by a model in which, from the first binary collisions of nucleus to the appearance of hadrons in the final state the system evolves hydrodynamicaly like a liquid of a very low viscosity.

I participate in the measurements of the long-range correlations are performed in the ATLAS experiment at the LHC. Observed is an azimuthal multiplicity correlation, customarily decomposed into the Fourier series

$$\frac{dN}{d\phi} \propto 1 + \sum_n v_n \cos n(\phi - \Psi_n),$$

where N is a number of particles, ϕ is an azimuthal angle, Ψ_n is a symmetry angle and v_n is an amplitude of the correlation or correlation strength. For n=2,3,.. the v_n are called elliptic, triangular, ... flow coefficients. The second coefficient, v_2, is related to the initial collision geometry while higher orders with the fluctuations in the initial geometry. The v_n's are in general functions of particle momenta, centrality and pseudorapidity. To measure the v_n, a multi-particle correlation methods are used. In the class of such methods, the Ψ_n is approximated by exploiting self-correlation of many particles, typically all measured in a subdetector, and particles correlated with it [3, 4]. The approximation is performed by estimating an average angle in a sub-detector (typically distant from the particle of interest to eliminate effects of short range correlations).

Using these methods ATLAS measured an integrated v_2 from lead-lead data collected in 2011 at the centre-of-mass energy per nucleon pair $\sqrt{s_{NN}} =$ 2.76 TeV. This, difficult experimentally, measurement proved to be more useful for comparisons with the theory than other previous results by other LHC experiments [5]. The main result is shown in the left panel of Figure 9 where the v_2 integrated over the entire transverse momenta spectrum is shown as a function of centrality percentile. I have also participated in preparation of a differential measurement of v_n from lead-lead collisions at the centre-of-mass energy per nucleon pair $\sqrt{s_{NN}} = 5.02$ TeV [6]. The v_n dependence on the charged particle transverse momenta is shown in the right panel of Figure 9.

Within the group analysing the heavy-ion data, besides the two mentioned analyses I was responsible for the development, preparation, and coordinations of the trigger from 2010 till 2017. I also serve in editorial boards which prepare conference notes and papers on behalf of the ATLAS collaboration [7, 8].

It needs to be stressed that in case of the ATLAS collaboration the conference notes and papers are thoroughly scrutinised inside the collaboration so that the published results are very high quality. The editorial boards play a crucial role in this process.

I have presented the heavy-ion results at several international conferences, among them the Recontres de Moriond (invited talk) or Quark Mat-

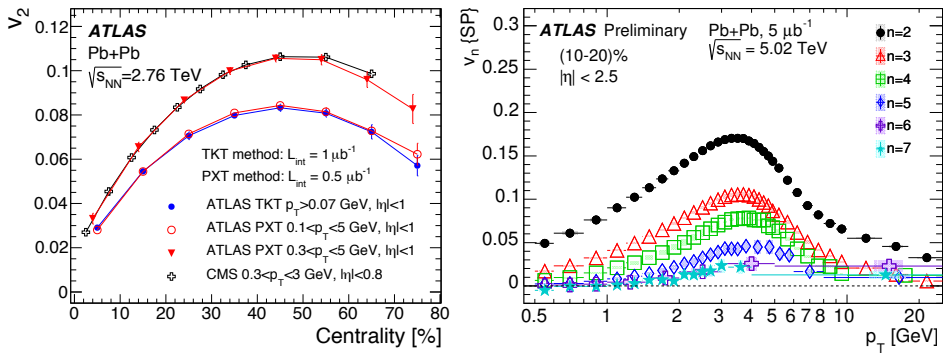

Figure 9: (left) Values of elliptic flow coefficient, v_2, as a function of collision centrality measured by the ATLAS experiment integrated over complete transverse momentum spectrum and compared to the CMS result. These measurements were performed on data from Pb+Pb collisions at the centre-of-mass energy per nucleon pair $\sqrt{s_{NN}} = 2.76$ TeV. Statistical and systematic uncertainties are denoted with the vertical bars [5]. (right) Values of flow coefficients v_n as a function of transverse momenta, p_T, for one centrality bin (10-20%) of Pb+Pb at centre-of-mass energy $\sqrt{s_{NN}} = 5.12$ TeV per nucleon pair [6].

ter [9, 10, 11, 12]. The later is a main conference in the field of ultra-relativistic heavy-ion collisions.

References

[1] Kovtun, P. et al. *Phys. Rev. Lett.*, 94:111601, 2005.

[2] RHIC Collaborations. *Nuclear Physics A (Special Issue)*, 757(1-2):1–283, 2005.

[3] A. M. Poskanzer and S. A. Voloshin. *Phys. Rev.*, C58:1671–1678, 1998.

[4] M. Luzum and J-Y. Ollitrault. *Phys. Rev.*, C87(4):044907, 2013.

[5] ATLAS Collaboration. Measurement of the centrality and pseudorapidity dependence of the integrated elliptic flow in lead-lead collisions at $\sqrt{s_{\rm NN}} = 2.76$ TeV with the ATLAS detector. *Eur. Phys. J.*, C74(8):2982, 2014.

[6] ATLAS Collaboration. Measurement of the azimuthal anisotropy of charged particles produced in 5.02 TeV Pb+Pb collisions with the ATLAS detector. Technical Report ATLAS-CONF-2016-105, CERN, Geneva, Sep 2016.

[7] ATLAS Collaboration. Measurement of charged particle spectra in pp collisions and nuclear modification factor $R_{\rm pPb}$ at $\sqrt{s_{NN}} = 5.02$TeV with the ATLAS detector at the LHC. Technical Report ATLAS-CONF-2016-108, CERN, Geneva, Sep 2016.

[8] ATLAS Collaboration. Azimuthal femtoscopy in central p+Pb collisions at $\sqrt{s_{\rm NN}} = 5.02$ TeV with ATLAS. Technical Report ATLAS-CONF-2017-008, CERN, Geneva, Feb 2017.

[9] T. Bold. Results from lead-lead collisions at $\sqrt{s_{NN}} = 2.76$ TeV with ATLAS at the LHC. In G. M. Bilei, S. Ciprini, and L. Fanò, editors, *Proceedings of the Physics at LHC 2011, Perugia, Italy, 2011*, volume eConf/C1106061, pages 59–62, 2012.

[10] T. Bold. Measurements of Elliptic Flow with the ATLAS Detector. *Nuclear Physics A*, 904:491c – 494c, 2013. Proceedings of Quark Matter Conference 2012.

[11] T. Bold. Soft Physics of p+Pb and Pb+Pb Collisions from the ATLAS Experiment at the LHC. *Acta. Phys. Pol. B*, 45(7):1331–1324, 2014.

[12] T. Bold. Heavy-ion measurements at ATLAS. In *Proceedings of the 51st Rencontres de Moriond on QCD and High Energy Interactions, La Thuile, Italy, 2016 (in preparation)*, 2016. Also available as tech. report ATL-PHYS-PROC-2016-043.

Tomasz Bold